RSC Advances

COMMUNICATION

View Article Online
View Journal | View Issue

Cite this: *RSC Adv.*, 2015, **5**, 70737

Received 8th July 2015
Accepted 12th August 2015

DOI: 10.1039/c5ra13407b

www.rsc.org/advances

Rapid manufacture of modifiable 2.5-dimensional (2.5D) microstructures for capillary force-driven fluidic velocity control†

Wenming Wu[ab] and Andreas Manz*[ab]

A cost-effective, straightforward and modifiable 2.5D microfabrication methodology, as we term multi-layer-tape lithography, is presented here for the first time. It uses a commercial scalpel to prototype 2.5D multilevel microchannels on commercial tape as thin as 500 μm in minutes. Three functional microfluidic devices are applied with this methodology, and display high performance regarding microdroplet formation, multiphase flux and self-powered sequential fluid delivery. We find the microchannel height of a 2.5D microchip can efficiently control capillary force-driven flow velocity. The autonomous sample flow rates through 55 mm long microchannels are 0.1 μL s^{-1}, 0.21 μL s^{-1} and 0.39 μL s^{-1} when multilevel microchannel heights are 200 μm, 300 μm, and 400 μm, respectively. After detachment of two, one, and one layers of tape from the three microchannels of a 2.5D tape-master, the microchannel heights are modified to 100 μm, 250 μm and 300 μm, with the autonomous sample flow rate changing to 0.03 μL s^{-1}, 0.15 μL s^{-1} and 0.28 μL s^{-1}, correspondingly. In contrast with 2D microfabrication technology, we anticipate that multi-layer tape lithography will pave the way for researchers, especially those from resource-limited labs, to develop cost-effective, practical, self-powered, and disposable 2.5D microfluidic devices.

1 Introduction

Ever since the micro Total Analysis System (μTAS) was introduced by us in 1990,[1] there has been an explosion of interest in facilitating miniaturized μTAS-based devices as cost-effective, portable, disposable and rapid lab-on-a-chip (LOC) systems for diagnostic, chemical or bio-medical Point-Of-Care (POC) analysis. An on-chip integrated self-powered micropump is a key element in the ideal POC diagnostic chip, which should be 'affordable, user-friendly, rapid and equipment-free', according to the World Health Organization.[2] Since the early 2000s, various promising self-powered pumping mechanisms have been developed for autonomous sample delivery inside the microsystem. In our previous works, several internally self-powered micropumps were successfully introduced to activate autonomous sample transport inside very long microchannels of PDMS glass, PMMA–PMMA and silicon-tubing microchips.[3–5] Other self-powered pumping mechanisms have also been developed to automate self-powered fluidic transport inside microchips, such as mechanical force-driven pumping,[6] capillary force-driven pumping,[7] wicking force-driven pumping[8,9] vapour force-driven pumping,[10] and degas-driven pumping,[11] *etc.* Lately, Lee's group presented seminal work on an automated self-powered sample flow (red dye) through implementing internally encapsulated working liquid plug (blue dye) inside a 2D microchip, wherein autonomous sample flow can be programmed to be 0.07 μL s^{-1}, 0.12 μL s^{-1} and 0.17 μL s^{-1}, simply by adjusting circular section angles of on-chip fibrous material by 20°, 40° and 60°, respectively.[2] This smart method, exempt from external off-chip operations, improves internally self-powered micropumping systems for potential POC applications. Yet besides the analytical channel functionalized for sample transport and POC detection, a working liquid channel and activation chamber (2.6 mm and 5 mm in width, respectively) should be integrated inside the same device to increase overall device size and systemic complexity. Nowadays, most self-powered micropumps are applied to 2D microchips. We estimate that if 2.5D microfluidic platforms are utilized for self-powered liquid transport instead of 2D platforms, performance regarding autonomously programmable liquid delivery may be improved. Inspired by this idea, we innovated a truly cost-effective, user-friendly, portable, disposable and rapid way to realize self-powered programmable sample delivery inside 2.5D microchips, integrating parallel multilevel analytical channels for autonomous liquid delivery of different rates in each channel. Simply by controlling the heights of analytical

[a]*Mechatronics Department, University of Saarland, Saarbrücken, Germany. E-mail: manz@kist-europe.de*

[b]*KIST Europe, GmbH, Campus E7.1, 66123 Saarbrücken, Germany*

† Electronic supplementary information (ESI) available. See DOI: 10.1039/c5ra13407b

channels, a similar autonomous programmable flow rate can be obtained as previously reported.[2]

The manufacturing efficiency of 2.5D microdevices is one key factor determining how widely such autonomously programmable liquid delivery methodology may spread to potential users. Currently speaking, rapid and inexpensive 2.5D microfabrication methodology is still a major challenge in the microfluidic field today. In classic 2.5D microfabrication methods, repeated micro-patterning such as multi-exposures by photolithography, multi-carvings by CNC micromachining, or multi-etchings by chemical etching are the most popular approaches in fabricating 2.5D microchannels with multiple heights, and are laborious and time-consuming. For instance, the 'stacking method' is one popular technique for fabricating 2.5D microchips today, wherein a first layer of photoresist should be prefabricated on substrate with accurate positioning, followed by repeated exposure, aligning and stacking of photoresist for the second, third, and fourth… layers, to finally form multiple-height 2.5D microchannels.[12,13] Because of the operational difficulty of accurate alignment on the micro-scale, very complicated 2.5D microstructures (*i.e.*, multilevel microchannels with more than five multi-level heights) are not eligible for the 'stacking method'. Lately, Cooksey and Atenciaab introduced a 'folding method' for fabricating 2D and 3D microdevices.[14] Nevertheless, this method is still inapplicable to multi-height 2.5D microstructures. A number of other 3D or 2.5D microfabrication methodologies have been proposed by our group[15–17] and other groups[18–20] recently. However, most of these approaches require expensive manufacturing equipment, time-consuming steps or labour-intensive operations, and are thus inaccessible to researchers from resource-limited laboratories. To solve the challenges associated with 2.5D microfabrication, herein a multiple-layer tape-based manufacturing methodology is introduced for the first time, wholly depending on benchtop and straightforward instruments. Microchannels as thin as 500 μm in width can easily be carved on multi-layer tape in minutes by a commercial scalpel. The number of tape layers can be calculated as 'microchannel height divided by the tape height'. After different layers of tape are detached from the microchannels, a 2.5D tape master consisting of multi-level microchannels can easily form, waiving the need for laborious alignment steps and expensive machineries. Ever since Whitesides *et al.* introduced PDMS for microfabrication in the late 1990s,[21,22] PDMS has become the most widely used material for microfabrication today. As a proof of concept, herein three PDMS microchips are treated with this multi-layer-tape lithographical methodology. In contrast to other microfabrication techniques,[23–31] multi-layer-tape lithography is more accessible to potential μTAS users limited to expensive microfabrication instrumentation, and displays further potential for application in a wide range of fields such as chemistry, biology, pharmacy and medicine, *etc.* (ESI 1†).

2 Experimental

2.1 Y-channel microchip

A schematic fabrication process of this 2.5D multi-layer-tape lithography is shown in Fig. 1. The channel height is determined by the number of tape (tesa 57176-00 tesapack ultra-strong tr. 66 m : 50 mm) layers attached to the glass slide, and can be conveniently adapted. The height of the tape is measured

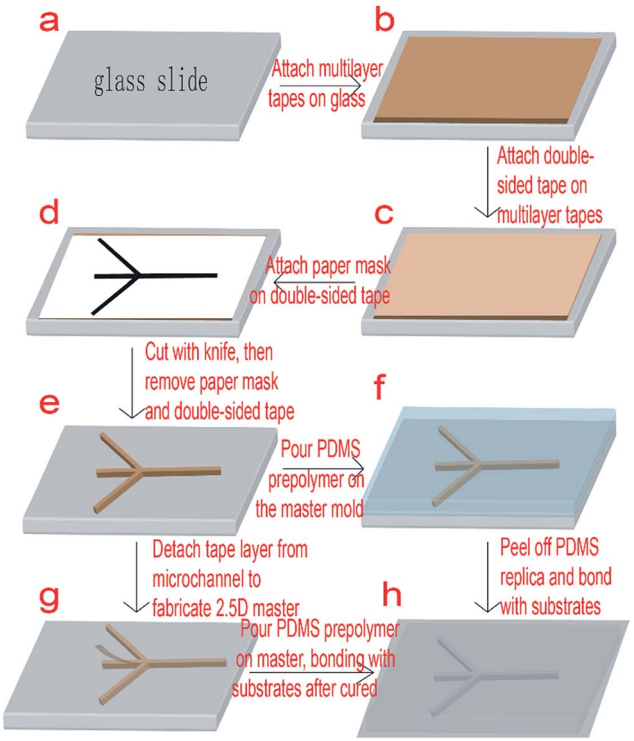

Fig. 1 Schematic steps of the multi-tape lithography for 2.5D microstructure fabrication. (a) The glass slide. (b) Multi-layer tape adheres to the glass slide. (c) Double-sided tape adheres to the multi-layer tape. (d) Paper mask is attached to the double-sided tape. (e) The multi-layer tape-master fabricated after removal of the paper mask. (f) After curing at 80 °C, for 30 min, the PDMS structure is peeled off. (g) A 2.5D master is made by detaching different layers of tape from each channel, according to the channel height. (h) PDMS replica is bonded with other substrates.

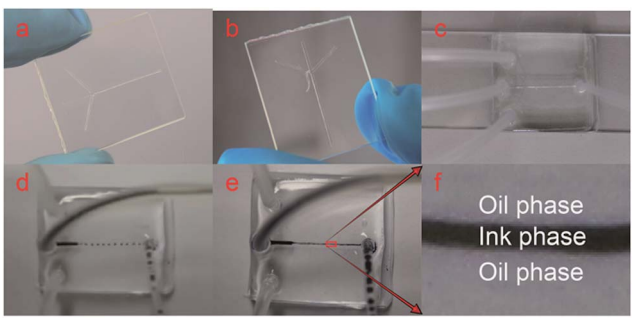

Fig. 2 (a) Three-layer tape-master, with a channel width of 500 μm and channel height of 150 μm. (b) One layer of tape is peeled off from the left channel of the tape-master in (a) to make a 2.5D tape-master. (c) The Y-structure PDMS chip fabricated by multi-layer-tape lithography. (d) Micro-droplet formation inside the Y-structure chip. The flow rates of ink and oil are 50 μL h^{-1} and 250 μL h^{-1}, respectively. (e) Multi-phase (oil-ink-oil) flow inside the Y-structure chip. The flow rates of ink and oil are 100 μL h^{-1} and 150 μL h^{-1}, respectively. (f) Magnification image of the multi-phase flow zone in (e), shown as a red rectangle.

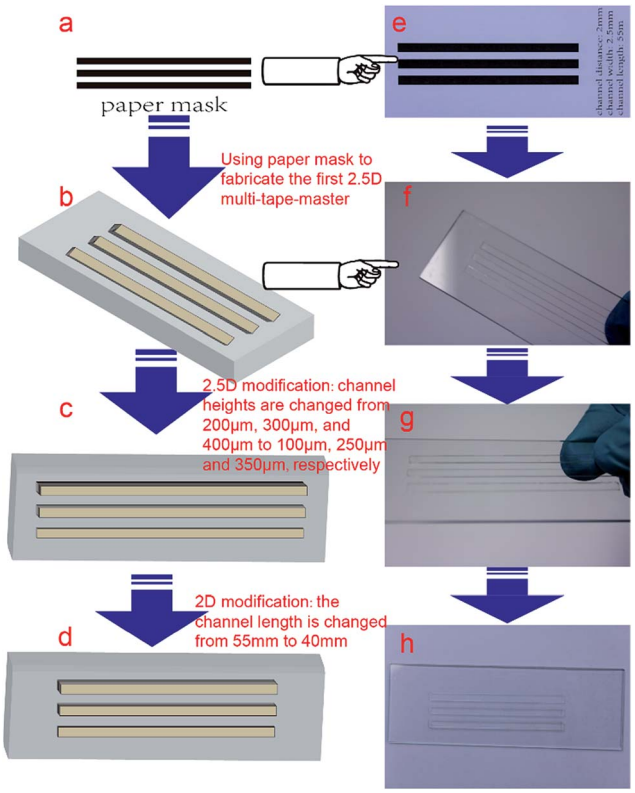

Fig. 3 The schematics for microchannel modification: 2D (channel length or width) and 2.5D (channel height) modifications of microstructure are done after the micro-device is fabricated. (a) The three-channel paper mask, with a channel length of 55 mm, channel distance of 2 mm, and channel width of 2.5 mm. (b) Original 2.5D tape-master with three parallel channel heights of 200 μm, 300 μm, and 400 μm, fabricated through multi-tape lithography. (c) One-time modifiable 2.5D tape-master, with three channel heights of 100 μm, 250 μm, and 350 μm, fabricated by directly modifying the multi-layer tape-master in (b). (d) Two-times modifiable 2.5D tape-master, with the same channel length of 45 mm, and three channel heights of 100 μm, 250 μm, and 350 μm, fabricated by directly modifying the tape-master in (c). (e) Real photo of paper mask. (f) Real photo of original tape-master. (g) Real photo of one-time modifiable tape-master. (h) Real photo of two-times modifiable tape-master.

by a Vernier calliper (Mitutoyo absolute digital). First, multiple layers of single-sided tape are attached to a paper mask (printed on an office printer) through double-sided tape (tesa double-sided tape 10 m : 15 mm) as shown in Fig. 1c. Second, the microstructure is cut into the tapes, with the paper mask and double-sided tape easily removed to leave a tape-glass hybrid master (Fig. 1e). After PDMS is poured in the master and cured (Fig. 1f), the PDMS replica can be taken off and bonded with a wide range of materials[23] (Fig. 1h) to make a functional chip. Tape layers in each channel can be detached depending on the required channel height to make the appropriate 2.5D structures (Fig. 1g).

We first fabricate one three-layer- tape-master (Fig. 2a) through this multi-layer-tape lithography, with a channel width of 500 μm and channel height of 150 μm. As shown in Fig. 2b, the tape layer can easily be detached from the 2D tape channel to fabricate a 2.5D tape-master. A Y-structure PDMS (Sylgard® 184) chip (Fig. 2c) is also fabricated from the multi-layer tape-master in Fig. 2a, with PDMS replica and glass substrate bonded by oxygen plasma (Diener electronic: 0010915) at a power of 75 W for 30 s. As shown in Fig. 2d and e, micro droplets and multiphase flow can stably form in this chip, demonstrating multi-layer tape lithography quantified for microfabrication. The quantified stable micro-droplet formation inside this chip is also provided in ESI 2,† promising a wide range of microdroplet-applicant downstream fields such as cultivation of mammalian cells,[32] controllable synthesis of nanoplates,[33] and interactional assay of cell pairs,[34] *etc.*

2.2 Parallel channel microchip

Furthermore, a 2.5D master containing three parallel channels with multi-level heights of 200 μm, 300 μm, and 400 μm, respectively, is fabricated by this 2.5D multi-layer tape lithography. To reveal the feasibility of the microstructural modifiability of this technique, modifications are realized to all three channels of the 2.5D tape-master, both in channel height (Fig. 3b, c, f and g) and in channel length (Fig. 3c, d, g and h). Tape layers of the three channels in Fig. 3b and f are four, six, and eight, respectively, corresponding to 200 μm, 300 μm, and 400 μm in channel height. Simply by detaching two, one, and one layers of tape from these three channels, we can change the multi-level channel heights to 100 μm, 250 μm, and 300 μm, finally. We also find that it is very easy to modify channels in the 2D level (width and length). As shown in Fig. 3c and d, after modification on three channels, the length of all channels changes from 55 mm to 45 mm. This proves that both 2D (channel length or width) and 2.5D (channel height) modification of the microstructure can be easily realized on the existing master, without the necessity of fabricating a new master.

3 Results and discussion

3.1 Programmable capillary flow

Two 2.5D microchips are fabricated from two tape-masters (Fig. 3f and g), with PDMS surface functionalized through oxygen plasma at 35 W for 0.7 min. We found programmable autonomous flow is easily produced in parallel 2.5D channels after sample injection (ESI 3†).

It requires about 4′35″, 3′20″, and 2′20″ for the ink flowing through three parallel channels of the first capillary flow chip (Fig. S1, ESI 4†), with multi-level heights of 200 μm, 300 μm, and 400 μm, respectively. Correspondingly, the autonomous sample flow rates through three 55 mm long microchannels are calculated to be 0.1 μL s^{-1}, 0.21 μL s^{-1} and 0.39 μL s^{-1}, respectively. Without the necessity of fabricating a new master, the second capillary flow chip is fabricated simply by detaching two, one, and one layers of tape from the three microchannels of the first 2.5D tape-master (Fig. 3f), with channel height changed to 100 μm, 250 μm, and 350 μm (Fig. 3g). As a result, total flowing-out time is changed to 7′50″, 3′55″, and 2′50″ (Fig. S2, ESI 4†), respectively. Correspondingly, autonomous sample flow rates

through three 55 mm long parallel microchannels are calculated to be 0.03 μL s^{-1}, 0.15 μL s^{-1} and 0.28 μL s^{-1}, respectively.

Quantitative analysis of autonomous flow distance (mm) is plotted against time (min), as indicated in Fig. 4. Because channel length (55 mm), channel width (2 mm), and surface functionalization (oxygen plasma at 35 W for 0.7 min) are all the same for three parallel multi-level microchannels, except for channel height, we can conclude that the sequential autonomous flow rate through these channels is dictated by channel height. As shown in Fig. 4, as the channel height increases, the flow rate becomes faster, and it displays the same trend in both the first capillary flow chip (Fig. S1, ESI 4†) and the second capillary flow chip (Fig. S2, ESI 4†). On the basis of the aforementioned analysis, we estimate a channel-height controlled autonomous programmable chip can be realized in accordance with the theoretical analysis, as illustrated in "Section 3.2".

3.2 Mathematical modelling

To theoretically verify the relationship between capillary flow rate and multi-level channel height, the fluidic hydrodynamic inside the 2.5D microchip is further analysed, wherein flowing velocity is determined by both the capillary driven force F_c and the capillary resistance force F_R. As shown in Fig. S3 of ESI 4,† F_c is in the same direction with the capillary flow, whereas F_R is in the opposite flow direction. The flowing velocity can be derived and calculated by the following equation,

$$F_c = F_R$$

If the micro-channel is a column with a circular cross-section, the flowing resistance force F_R can be calculated by the Hagen–Poiseuille equation:

$$-\frac{dp_l}{dz} = \frac{8\eta u}{r^2}$$

where η is the viscosity of the liquid, p_l is the internal pressure of the liquid medium which is proportional to the flowing resistance force, u is flowing velocity, and r is radius.

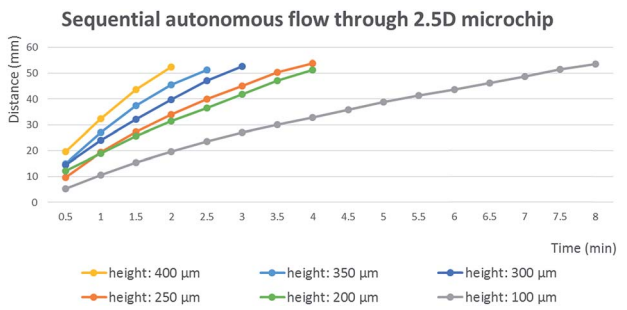

Fig. 4 Quantitative analysis of sequential autonomous flow inside 2.5D microchips with multi-level channel height of 100 μm (grey dotted line), 200 μm (green dotted line), 250 μm (henna dotted line), 300 μm (deep blue dotted line), 350 μm (light blue dotted line) and 400 μm (brown dotted line), respectively. Channel length and width are 2 mm and 55 mm, respectively.

From this equation, we can estimate that the velocity is in proportion to the square of the diameter of the column microchannel. In other words, the flowing-out time decreases as the column microchannel diameter increases.

However, the cross-section of the channel here is rectangular instead of circular. In previous work, we have systemically analysed the relationship between the flowing resistance force and the flowing velocity inside a channel with a rectangular cross-section, which is the same channel type as used here, and it can be represented by the following equation,[28]

$$-\frac{dp_l}{dz} = \frac{\lambda\rho u^2}{2d_h}$$

where λ is a frictional coefficient of capillary-driven flow, ρ is liquid density, u is flowing velocity, and d_h is the equivalent diameter of the rectangular microchannel.

It is easily seen that, as the channel height increases, d_h will increase, resulting in decreased resistance force. Therefore the flowing velocity should increase if the channel height increases, resulting in decreased flowing-out time.

3.3 Microchannel characterization

We further use a scanning electronic microscope (QUANTA FEG250) and optical microscope (Zeiss axiovert S100) to characterize the surface smoothness of 2.5D tape-masters. Multi-level tape layers of 3, 5, 7 and 11, as well as intersectional multiple tape layers of 11–10 and 4–3, are selected for characterizing both the top surface and the cross-sectional surface. As shown in Fig. 5a–c, the top surface of the tape-master displays qualified smoothness, comparable to the surface of a glass slide. At 16 000× magnification, dot-like structure as little as 100 nm is found (Fig. S4, ESI 4†), proving roughness at top surface of the multi-layer tape-master is ignorable at micro-meter scale. However, the smoothness of the boundary surfaces in the multi-layer tape-master depends on the height of the tape in use. There are some curved grooves between tape layers, which are around 10 μm in height, as shown in Fig. 5a–c. To better reveal these curved grooves, the cross-section of the multi-layer tape-master is further characterized (Fig. 5d–f). Because the multi-layer 2.5D tape-master is built up of a single layer of tape as a constructional unit, the tape layer is visible and has about 10 μm high curved grooves in between, as shown in Fig. 5d and f. Intersectional height decrease of 2.5D tape-master is also characterized in Fig. 5e and f, wherein one layer of tape is detached in intersectional locations to produce a reduction of channel height by 50 μm from left to right in both cases.

Similarly to photolithography-based master prototyping wherein proper photoresist (*e.g.*, SU-8 2005, SU-8 2007, SU-8 2010 or SU-8 2015, *etc.*) should be selected depending on the specialized microchannel height, herein suitable tape (10 μm, 50 μm, 100 μm, in height *etc.*) should also be dependent on microchannel height. In our case, the height of all microchannels (Fig. 2 and 3) are within 400 μm, so tape 50 μm in height (tesa 57176-00 tesapack ultra-strong tr. 66 m : 50 mm) is appropriate for prototyping microchannels. Nevertheless, if a

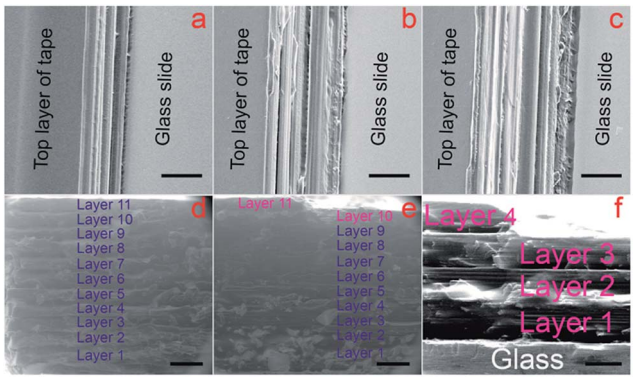

Fig. 5 The SEM image of the tape-master. (a) The boundary of a three-layer tape channel. (b) The boundary of a five-layer tape channel. (c) The boundary of a seven-layer tape channel. (d) The cross-section of an 11-layer tape channel. (e) The cross-section of the 11-layer and 10-layer tape channel. (f) The cross-section of the four-layer and three-layer tape channel. Rule bars are 125 μm in (a–c); 100 μm in (d and e); and 50 μm in (f).

master with channel height lower than 50 μm should be fabricated, then the selected tape height should be less than 50 μm, such as 10 μm or 25 μm. The height of the tape also affects the resolution of the channel height of the microchip. For example, if two kinds of single-sided tape with heights of 10 μm and 15 μm are selected, then a height resolution of 5 μm can be realized, because a channel height of 10 μm, 15 μm, 20 μm, and 25 μm… *etc.*, can be fabricated simply by arranging these two kinds of tape.

4 Conclusion

This paper reports a multi-layer tape lithography for fabricating 2.5D microchips easily, rapidly and cheaply. Without any expensive instruments or reagents, the total manufacturing cost of a 2.5D master by multi-layer tape lithography is under 0.03 US$, allowing convenient microstructural modification of the tape-master in both 2D level (channel length is modified by 10 mm here) and 2.5D level (channel heights are modified by 50 μm and 100 μm here). If we use a commercial scalpel to manually cut microchannels in the multi-layer tape, the smallest microchannel width is 500 μm. A Y-shaped microchannel as thin as 500 μm in width is directly fabricated through a manual knife-cut, quantified for microdroplet formation when the flow rates of ink phage and oil phage are 50 μL h^{-1} and 250 μL h^{-1}, respectively, and multi-phage flow when the flow rates of ink and oil are 100 μL h^{-1} and 150 μL h^{-1}, respectively.

Sequential and programmable autonomous flow is realized in 2.5D microchips fabricated through this multi-layer tape lithography. Two 2.5D capillary force-driven flow chips are fabricated, with channel heights controlled to be 200 μm, 300 μm, and 400 μm for the first chip, and 100 μm, 250 μm, 350 μm for the second chip. The flowing-out time of ink in 55 mm long channels increases from 2′20″ to 7′50″ as the height of channel decreases from 400 μm to 100 μm, suggesting that the channel height is an efficient approach for controlling the capillary flow rate, as supplementary of previous methods relying on a 2D microchip. Through mathematical modelling, the relationship between microchannel height and autonomous capillary flow rate is also systemically studied, verifying that autonomous capillary flow rate increases as the multilevel microchannel increases in height, in accordance with experimental results.

Given the aforementioned advantages, we believe that multi-layer tape lithography can dramatically decrease the microfabrication expense of 2.5D microdevices and thus lower the barrier to the widespread use of microfluidic POC chips in non-engineering labs or automatic analysis labs, which may be unable to afford expensive clean rooms, UV transmitters or inkjet printer, *etc.*

References

1 A. Manz, N. Graber and H. M. Widmer, *Sens. Actuators, B*, 1990, **1**, 244.
2 T. Kokalj, Y. Park, M. Vencelj, M. Jenko and L. P. Lee, *Lab Chip*, 2014, **14**, 4329.
3 W. Wu, K. T. L. Trinh and N. Y. Lee, *RSC Adv.*, 2015, **5**, 12071.
4 W. Wu, K. T. L. Trinh and N. Y. Lee, *Analyst*, 2012, **137**, 983.
5 W. Wu, K. T. L. Trinh and N. Y. Lee, *Analyst*, 2015, **140**, 1416.
6 H. Hwang, S.-H. Kim, T.-H. Kim, J.-K. Park and Y. Kyoung, *Lab Chip*, 2011, **11**, 3404.
7 P. Novo, F. Volpetti, V. Chu and J. P. Conde, *Lab Chip*, 2013, **13**, 641.
8 B. Lutz, T. Liang, E. Fu, S. Ramachandran, P. Kauffman and P. Yager, *Lab Chip*, 2013, **13**, 2840.
9 G. M. Whitesides, *Lab Chip*, 2013, **13**, 4004.
10 S. Begolo, D. V. Zhukov, D. A. Selck, L. Li and R. F. Ismagilov, *Lab Chip*, 2014, **14**, 4616.
11 I. K. Dimov, L. Basabe-Desmonts, J. L. Garcia-Cordero, B. M. Ross, A. J. Ricco and L. P. Lee, *Lab Chip*, 2011, **11**, 845.
12 D. T. Chiu, E. Pezzoli, H. Wu, A. D. Stroock and G. M. Whitesides, *Proc. Natl. Acad. Sci. U. S. A.*, 2001, **98**, 2961.
13 M. Zhang, J. Wu, L. Wang, K. Xiao and W. Wen, *Lab Chip*, 2010, **10**, 1199.
14 G. A. Cooksey and J. Atenciaab, *Lab Chip*, 2014, **14**, 1665.
15 W. Wu and N. Y. Lee, *Anal. Bioanal. Chem.*, 2011, **400**, 2053.
16 W. Wu and N. Y. Lee, *Sens. Actuators, B*, 2013, **181**, 756.
17 W. Wu, K. T. L. Trinh and N. Y. Lee, *Analyst*, 2012, **137**, 2069.
18 P. K. Yuen and V. N. Goral, *Lab Chip*, 2010, **10**, 384.
19 W. Lee, D. Kwon, W. Choi, G. Y. Jung and S. Jeon, *Sci. Rep.*, 2015, **5**, 7717.
20 M. Zhang, J. Wu, L. Wang, K. Xiao and W. Wen, *Lab Chip*, 2010, **10**, 1199.
21 J. C. McDonald, D. C. Duffy, J. R. Anderson, D. T. Chiu, H. Wu, O. J. A. Schueller and G. M. Whitesides, *Electrophoresis*, 2000, **21**, 27.
22 G. M. Whitesides, E. Ostuni, S. Takayama, X. Jiang and D. E. Ingber, *Annu. Rev. Biomed. Eng.*, 2001, **3**, 335.
23 W. Wu, J. Wu, J. H. Kima and N. Y. Lee, *Lab Chip*, 2015, **15**, 2819–2825.

24 T. Kwa, Q. Zhou, Y. Gao, A. Rahimian, L. Kwon, Y. Liu and A. Revzin, *Lab Chip*, 2014, **14**, 1695.
25 R. L. Hartman, H. R. Sahoo, B. C. Yen and K. F. Jensen, *Lab Chip*, 2009, **9**, 1843.
26 P. Vulto, P. Kuhn and G. A. Urbanb, *Lab Chip*, 2013, **13**, 2931.
27 L. Zhang, W. Wang, X. Ju, R. Xie, Z. Liu and L. Chu, *RSC Adv.*, 2015, **5**, 5638.
28 W. Wu, K. T. Kang and N. Y. Lee, *Analyst*, 2011, **136**, 2287.
29 J. Kim, R. Surapaneni and B. K. Gale, *Lab Chip*, 2009, **9**, 1290.
30 X. Fang, S. Wei and J. Kong, *Lab Chip*, 2014, **14**, 911.
31 A. D. ávan der Meer, P. Dijke and A. den Berg, *Lab Chip*, 2013, **13**, 3562.
32 H. Hufnagel, A. Huebner, C. Gülch, K. Güse, C. Abell and F. Hollfelder, *Lab Chip*, 2009, **9**, 1576.
33 Q. Fu, G. Rana and W. Xu, *RSC Adv.*, 2015, **5**, 37512.
34 T. P. Lagus and J. F. Edd, *RSC Adv.*, 2013, **3**, 20512.